SCIENTIFIC REP🝊RTS

OPEN

Spatio-temporal patterns of stream methane and carbon dioxide emissions in a hemiboreal catchment in Southwest Sweden

Sivakiruthika Natchimuthu[1], Marcus B. Wallin[2,3], Leif Klemedtsson[4] & David Bastviken[1]

Global stream and river greenhouse gas emissions seem to be as large as the oceanic C uptake. However, stream and river emissions are uncertain until both spatial and temporal variability have been quantified. Here we investigated in detail the stream CH_4 and CO_2 emissions within a hemiboreal catchment in Southwest Sweden primarily covered by coniferous forest. Gas transfer velocities (k_{600}), CH_4 and CO_2 concentrations were measured with multiple methods. Our data supported modelling approaches accounting for various stream slopes, water velocities and discharge. The results revealed large but partially predictable spatio-temporal variabilities in k_{600}, dissolved gas concentrations, and emissions. The variability in CO_2 emission was best explained by the variability in k, while dissolved CH_4 concentrations explained most of the variability in CH_4 emission, having implications for future measurements. There were disproportionately large emissions from high slope stream reaches including waterfalls, and from high discharge events. In the catchment, stream reaches with low slope and time periods of moderate discharge dominated (90% of area and 69% of time). Measurements in these stream areas and time periods only accounted for <36% of the total estimated emissions. Hence, not accounting for local or episodic high emissions can lead to substantially underestimated emissions.

Inland waters emit significant amounts of greenhouse gases such as methane (CH_4) and carbon dioxide (CO_2) to the atmosphere[1–6]. Despite their low areal coverage, streams are one of the most important contributors to the total aquatic CO_2 emissions and the estimated global CO_2 emissions from streams and rivers (1.8 Pg C yr^{-1}) exceed the corresponding emissions from lakes and reservoirs (0.3 Pg C yr^{-1})[2]. Moreover, global stream CO_2 emissions are in the same order of magnitude as the estimated land C sink of 2.6 Pg C yr^{-1} or oceanic C uptake of 2.3 Pg C yr^{-1}[7]. The disproportionately large contribution from streams is partly a function of higher concentrations of CO_2 observed in streams than in lakes[8,9]. The gas transfer velocities (k) observed in streams are also usually higher than in lakes due to the turbulence generated when water is moving along a stream channel. Consequently, some of the highest reported k values have been observed in small streams[3]. Even though stream emissions appear to be large contributors to landscape aquatic CO_2 budgets with high per m^2 emissions[10], they are often neglected in landscape level carbon budgets due to the lack of data. Furthermore, stream CH_4 emissions are poorly understood although there is a growing awareness of their importance[11,12]. Global stream emissions have been estimated to be 27 Tg CH_4 yr^{-1} by Stanley *et al.*[6] and it has been suggested that CH_4 emissions from streams could be even more variable in space and time than CO_2 emissions[6,13].

Previous stream emission estimates often rely on data with poor resolution in space and time. Yet, stream emissions are known to be very variable. The spatial variability in gas emissions has been linked to highly variable k which is a result of e.g. stream channel morphology, channel slope, water velocity etc.[14–16]. In addition, dissolved gas concentrations along a stream network are also often highly variable as a result of both gas input (influenced by surrounding land-use including upstream wetlands, soil characteristics, groundwater inputs, etc.[5,11,17–22]), and gas loss (dependent on k which regulates the vertical gas exchange[13]). Furthermore, temporal variations in gas

[1]Department of Thematic Studies–Environmental Change, Linköping University, 581 83 Linköping, Sweden. [2]Department of Earth Sciences, Uppsala University, 752 36 Uppsala, Sweden. [3]Department of Ecology and Genetics/Limnology, Uppsala University, 752 36 Uppsala, Sweden. [4]Department of Earth Sciences, University of Gothenburg, 405 30 Gothenburg, Sweden. Correspondence and requests for materials should be addressed to S.N. (email: sivakiruthika.natchimuthu@liu.se)
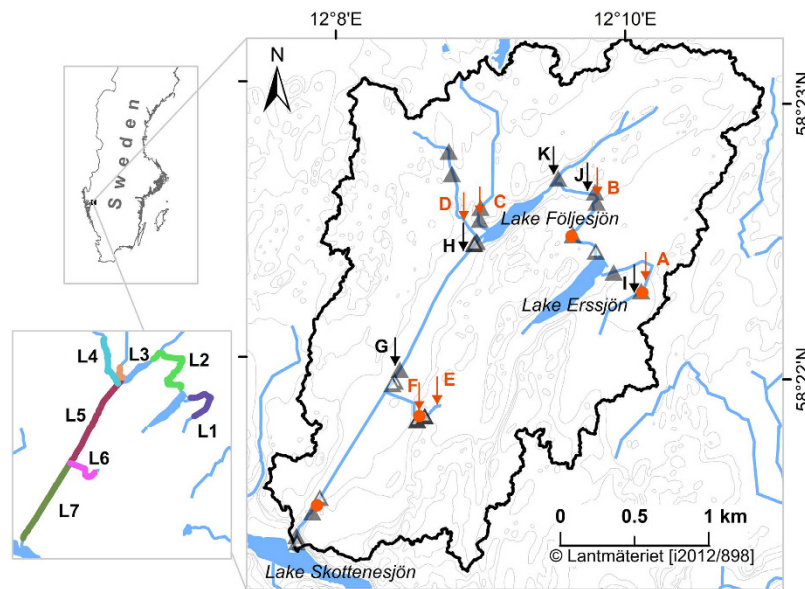
Figure 1. A map of the Skogaryd Research Catchment (SRC) showing the studied streams, the catchment boundaries and sampling locations. Red arrows denote the reaches (**A–F**) where propane injections were made and the triangles denote the locations of CO_2 sensor chambers (open triangles–2012, closed triangles–2013). Black arrows (G–K) denote points where CO_2 emissions were directly measured for validation using the drifting/floating chamber method (see Supplementary Information). The locations of the four discharge monitoring stations are given as red circles. The inset map shows the different location categories (L1–L7) made for the purpose of describing spatial variability. The figure was created with ArcMap 10.3.1 available from http://www.esri.com/. The background map was obtained from Lantmäteriet (National Land Survey of Sweden) and published under the copyright agreement i2012/898 with Linköping University.

concentrations and emissions have been linked to variations in stream discharge[23,24]. A variable discharge causes changes in the ground water level and hence the input of gases to the stream[17,25]. Discharge events like snow melt and rainstorm events can have a rapid effect on the stream gas concentrations and emissions either due to dilution or increased supply of dissolved gases[12,25–27]. Variability in discharge could also affect the *k* through changes in turbulence which affect the emissions[15]. Diel cycles in CO_2 concentrations as a result of photosynthesis and/or mineralisation processes have also been recorded in streams[18,28]. Thus, large spatio-temporal variability in stream gas emissions could be expected while the present data rarely allow analysis of how this variability influences yearly stream network emissions. Therefore, there is a need for long-term studies of whole catchment stream network greenhouse gas emissions including both spatial and temporal dimensions.

Another dilemma is that most large scale aquatic CO_2 emission estimates are based on indirect methods where CO_2 is estimated using temperature, pH and total alkalinity[2,29]. Such indirect methods have now been shown to overestimate CO_2 concentrations, in organic rich, acidic, or low alkalinity waters[30]. There have been attempts to reduce this bias by not considering data from water with a pH below 5.4[2,29]. This resolves some dilemmas but also means that acid waters were not accounted for. In any case, indirect estimates of concentrations lead to great uncertainties and more data from direct, continuous measurements are needed. Accordingly, a growing number of recent large scale studies also focus on direct methods to measure concentrations[5,19–21]. In this study we combined direct measurements of *k* (using a tracer gas approach) with direct determination of CH_4 and CO_2 concentrations during a two-year study period in the stream network of a hemiboreal catchment in Southwest Sweden (Fig. 1). The overall aim was to assess and account for spatio-temporal dynamics when estimating stream network CH_4 and CO_2 emissions. To do this we (1) measured the spatio-temporal variability in *k* in key reaches of the stream network (2) used the measurements to develop a locally validated model for *k* for the whole stream network (3) derived stream network CH_4 and CO_2 emissions from directly measured concentrations and the modelled *k,* accounting for the identified spatio-temporal variability and (4) quantified the importance of turbulent sections and high discharge periods.

Results

Measured and modelled gas transfer velocities. Gas transfer velocities (*k*) depend on the diffusivity of the gas and the temperature influencing the viscosity of the water. Hence, *k* values are related to Schmidt numbers representing the ratio of the kinematic viscosity of water to the diffusion coefficient of the gas in focus. For comparison across temperatures and gases, k_{600}, representing *k* normalised to a Schmidt number of 600 (corresponding to the Schmidt number for CO_2 at 20 °C[31]), is often used. The k_{600} measured in six stream reaches using propane injections ranged from 0.2 to 558.7 m d^{-1}, respectively (Table 1). Reaches characterised by steep sections and waterfalls (B, C, and F in Fig. 1) had much higher k_{600} than reaches having almost straight channels with flat

	A	B	C	D	E	F
Catchment area (km^2)	0.6	1.5	0.4	0.5	0.4	0.5
Length (m)	34	32	54	31	20	24
Slope (%)	1.5	7.5	7.6	0.5	0.3	19.3
Mean width (m)^a	0.9–1.1	0.8–2.4	0.7–0.9	0.5	0.7–1.3	0.7
Mean depth (m)^a	0.08–0.2	0.09–0.4	0.09–0.2	0.2	0.1–0.4	0.1
Reach area (m^2)^a	31.6–40.5	24.4–77.6	37.4–46.7	16.8	13.4–28.2	16.9
Discharge (L s^{-1})	27.6 (6.5–101.2)	82.8 (5.2–274.7)	23.2 (8.5–58.4)	10.1	30.2 (4.5–117.4)	7.3
Reach travel time (min)	3.4 (1.5–5.1)	2.4 (0.7–5.7)	4.4 (1.9–6.4)	3.9	2.6 (0.8–4.0)	3.2
Mean velocity (m s^{-1})	0.2 (0.1–0.4)	0.3 (0.09–0.7)	0.3 (0.1–0.5)	0.1	0.2 (0.08–0.4)	0.1^b
Water temperature (°C)	9.2 (5.5–15.2)	9.7 (5.6–17.2)	8.4 (6.8–12.9)	5.8	8.4 (5.2–13.3)	6.4
k_{600} (m d^{-1})	10.7 (2.6–27.5)	152.6 (13.9–558.7)	72.5 (37.1–185.7)	3.0 (2.2–4.4)	1.2 (0.2–3.5)	73.7 (71.7–75.3)
n^c	12 (5)	15 (5)	12 (4)	3 (1)	8 (5)	3 (1)

Table 1. Stream characteristics given as the mean (or minimum–maximum) of physical parameters of the studied reaches and k_{600} measured using propane injections. ^{a}Range of mean width, depth and area of the reaches, except for reaches D and F where measurements were done once. ^{b}Although the slope in reach F was the highest, on the measurement day the discharge was very low and thus generated low velocity value. ^{c}Number of observations of k_{600}; the number of propane injections in each reach is given in the brackets (reaches D and F were sampled once).

Model no.	Regression equation	n	Adjusted R^2	p	MSE^a
1	Log$_{10}$V = −1.323 + (0.466 × log$_{10}$ D) + (0.056 × log$_{10}$S)	21	0.91	<0.001	0.006
2	Log$_{10}$ k_{600} = 0.319 + (2.110 × V) + (1.026 × log$_{10}$S)	53	0.92	<0.001	0.050

Table 2. Regression equations predicting stream velocity (V, in m s^{-1}) from discharge (D, in L s^{-1}) and slope (S, in %), and k_{600} (m d^{-1}) from stream velocity and slope. ^{a}Mean square error of the regression.

topography (A, D and E in Fig. 1, see Table 1 for mean and ranges). Additional description of the results from the propane injections is given in the Supplementary Information.

Bivariate relationships between k_{600} and discharge or water velocity were strong for reaches with higher slopes but were weak or absent in the flatter reaches (Fig. S1; see details on velocity estimation in the Supplementary Information). However, multiple linear regression models of k_{600} as a function of water velocity and slope generated strong relationships with adjusted R^2 of 0.92 ($p < 0.001$; Table 2), and a close correspondence between predictions and observations for k_{600} (Fig. 2). However, the model slightly overestimated k_{600} in the higher range. To correct this, we multiplied the modelled k_{600} by a factor of 0.89 obtained from the slope of the linear regression between measured and modelled values (Fig. 2b). This corrected model was used to estimate daily k_{600} for all reaches of the stream network. The division of the stream network into 84 reaches, each covering a change in elevation of 0.5 m, is described in the Supplementary Information. The reaches were longer in flat areas and shorter in steep areas of the catchment and this definition of reaches was useful to characterise spatial variability in emissions as shown later. When estimating k_{600}, the models were applied only in the velocity range covered by the k measurements i.e. up to a velocity of 0.7 m s^{-1}. Only 2% of the days had an average reach velocity that was above this limit and during these time periods the reach specific maximum k_{600} was used.

The mean modelled k_{600} for the entire stream network was 21.3 ± 64.8 m d^{-1} (median was 4.6 m d^{-1}; $n_{modelled} = 51133$; Fig. S2). A few steep reaches in the stream network displayed very high k_{600} and thus skewing the mean k_{600} for all reaches (Figs S3 and S4). The mean modelled k_{600} differed widely between locations and slope categories (General Linear Model (GLM), $p < 0.001$; Fig. S4; see Methods for categories) highlighting a large spatial variability. The mean k_{600} from location L7 (see Fig. 1), which has a steep elevation with waterfalls before entering lake Skottenesjön, was more than 3 times higher than the overall mean. Location L5, which represents a relatively flat area of the catchment with low water velocity, had the lowest mean k_{600} (Fig. S4). The slope category S5, including the steepest reaches, had 5 times higher mean k_{600} than the overall mean (Fig. S4; Table 3).

The modelled k_{600} values were also highly variable in time. The modelled mean k_{600} from the highest discharge periods (greater than four times the mean daily discharge) was more than 3 times higher than the overall mean modelled k_{600} from the two years (Table 3). In particular, flooding events in the reaches with higher slope could result in an up to 7-fold increase in k_{600} (Fig. S5). Moreover, there was an inter-annual variability in k_{600} with 1.4 times higher k_{600} in 2014 than in 2013 (Fig. S5).

Spatio-temporal variability in CH$_4$ concentrations.

The stream water CH$_4$ concentrations were highly variable and with a mean concentration of 1.7 ± 3.5 [0.01–46.1] μM (mean ± 1 SD [min − max]). For comparison, the theoretical CH$_4$ concentration in equilibrium with the atmosphere (2.0 ± 0.09 ppm measured during the study) was 0.004 μM. Hence, CH$_4$ was detected in all of our samples with concentrations that were more than 2
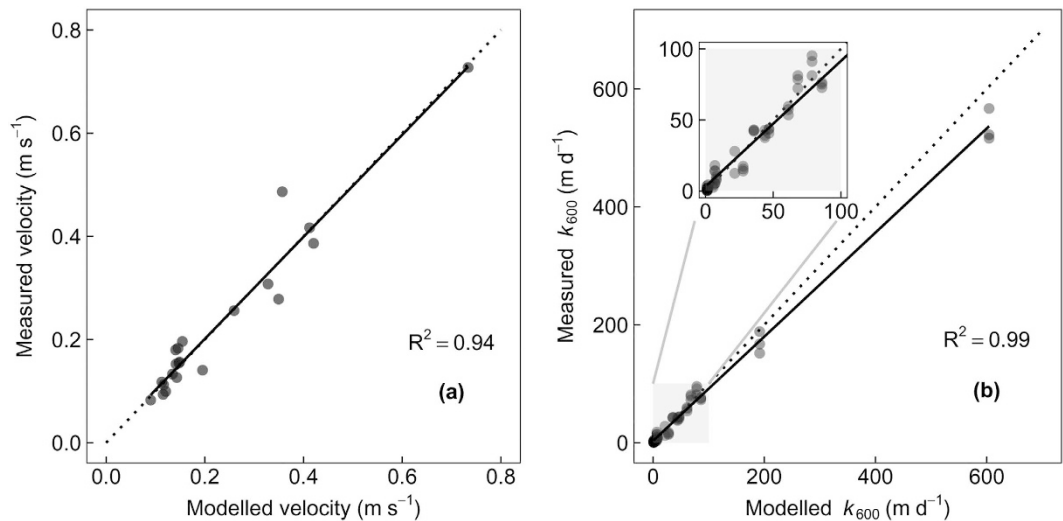
Figure 2. Scatter plots of modelled velocity (**a**) and k_{600} (**b**) against the corresponding measured values. All p values were < 0.001. The insets in panel (**b**) shows the fit in the lower range of k_{600}. The modelled k_{600} was multiplied by a factor of 0.89 to avoid overestimates in higher ranges of modelled values (see text). Darker symbol colour indicates data point overlaps.

Slope category[a]	Percent area (%)[b]	CH_4 emission ratio[c]	CO_2 emission ratio	k ratio
S1	90.5	0.2	0.2	0.1
S2	5.2	0.7	0.4	0.3
S3	2.6	1.5	1.4	1.0
S4	0.7	1.9	2.3	1.7
S5	0.9	3.1	3.8	5.1
Discharge ratio[d]	**Percent occurrence (%)[e]**	**CH_4 emission ratio**	**CO_2 emission ratio**	**k ratio**
<1	69.0	0.6	0.5	0.5
1 to 2	15.7	1.2	1.4	1.5
2 to 3	5.9	2.0	2.4	2.6
3 to 4	4.2	2.4	2.7	2.8
>4	5.1	3.2	4.0	3.3

Table 3. Ratio of mean emissions and k from different slope and discharge categories to the overall mean values indicating under or overestimates if only a single slope and discharge category is considered. Ratios <1 denote underestimate and >1 denote overestimate. [a]Slope of reaches divided into five categories; S1 (0–1%), S2 (1–2%), S3 (2–4%), S4 (4–6%) and S5 (6–21%). [b]Mean percentage of area of each slope category. [c]Emission estimates relative to whole-catchment mean; for example, a ratio of 1.5 means that the emission from the particular slope or discharge category was 1.5 times higher than the whole-catchment mean. [d]Ratio of discharge to the mean reach discharge from each reach was calculated and divided into five categories for comparison. [e]Percentage of time with the corresponding discharge ratios during the study period.

to over 11000 times supersaturated relative to atmospheric levels. The mean CH_4 concentrations in the sampling points of L1, L4 and L5 were similar and higher than the mean stream concentration (GLM, $p < 0.001$; Fig. 3). The sampling points in L2 and L7 had similar concentrations near the overall mean. The samples from L6 showed the lowest CH_4 concentrations (Fig. 3). The mean CH_4 concentration in samples from the slope category S1 was significantly higher than S3, S4 and S5 but similar to S2 (Fig. 3). The mean concentration in S5, which had the highest water velocity, was lower than all other slope categories.

The CH_4 concentrations showed large temporal variations (Fig. S6). However, CH_4 concentrations had weak or no correlations with the variables investigated (water temperature, velocity, discharge and k values for CH_4; all variables, measured at multiple locations in space, were normalised to the 2-year mean for each location to remove spatial variability when testing for temporal correlations).

Spatio-temporal variability of CO_2 concentrations. The mean stream water CO_2 concentration was 131.6 ± 79.8 [range 27.5–1124.1] μM (corresponding to 2463 ± 1546 [520–22118] μatm when expressed as partial pressure of CO_2). These concentrations correspond to excess concentrations of 1.3 to 54 times when compared to atmospheric levels (mean atmospheric CO_2 concentration of 405 ± 28 ppm measured during the study). All
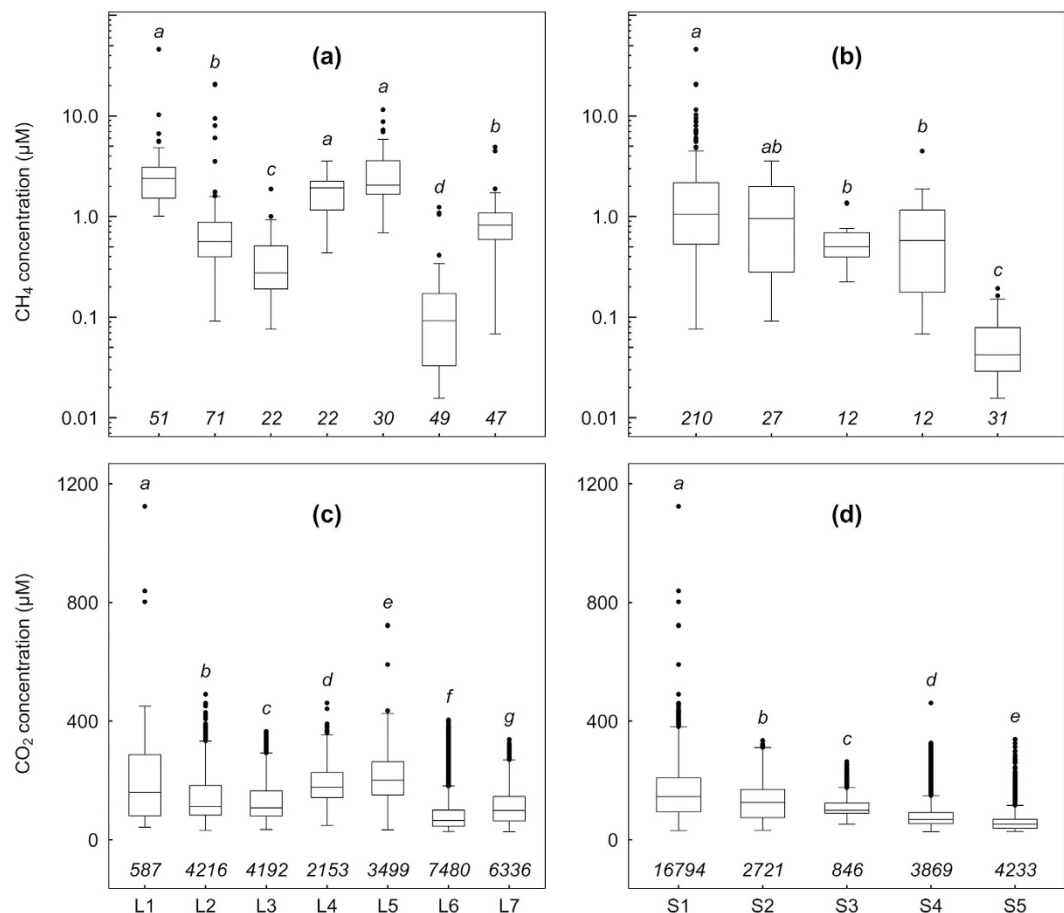
Figure 3. Boxplots of CH_4 (**a**,**b**) and CO_2 (**c**,**d**) concentrations measured in the streams grouped into location and slope categories. The boxes show quartiles and the median, the whiskers denote data within 1.5 times of the interquartile range and the black closed circles denote data values outside the interquartile range. The letters above the boxes represent Tukey's post-hoc test and boxes with different letters had significantly different concentrations ($p < 0.05$). The numbers below the boxes are the number of measurements in each category. Note the $\log_{10}$ scale in y-axis of panels (**a**,**b**). The concentrations in equilibrium with atmospheric concentrations are 0.004 μM and 23.5 μM for CH_4 and CO_2, respectively.

our measurements showed that the streams were supersaturated relative to the atmosphere at all times. The CO_2 concentrations occasionally reached higher than 15000 μatm (approx. >670 μM) especially close to the inlets and outlets of the lake Följesjön. In general, the spatial variability in CO_2 was lower than for CH_4 (Fig. 3). Location category L6 had the lowest mean CO_2 (GLM; $p < 0.001$; Fig. 3). The mean CO_2 concentrations in L1, L4 and L5 were 1.4, 1.4 and 1.6 times higher than the overall mean stream CO_2 and the mean concentrations in L2 and L3 were close to the overall mean (Fig. 3). If instead organizing data based on slope category, the mean CO_2 concentration in the slope category S1 was 1.2 times higher than the mean stream CO_2 and, as for CH_4, the CO_2 concentrations were lowest in slope category S5 (Fig. 3). Local measurements upstream and downstream of steep stream sections/waterfalls showed that CO_2 concentrations were consistently lower downstream due to the high turbulence causing a rapid loss of CO_2 over a short distance (see Fig. S7 for an example).

The temporal variability in CO_2 concentration was complex (Figs S6 and S7) and no clear relationships with discharge were found. High discharges increased the CO_2 in some periods, but not consistently. During the dry periods, small pools of standing water were formed in the streams and had a relatively high CO_2. High discharges after these dry periods sometimes diluted the CO_2.

Biweekly CO_2 and CH_4 concentrations were not correlated in time (after normalisation to remove spatial variability; Pearson's $r = -0.054$, $p = 0.57$). Diel variability in CO_2 concentration was frequently observed from the high resolution CO_2 sensor data (Fig. S7). CO_2 concentrations had weak or no correlations with the tested variables water temperature, velocity, discharge and k values for CO_2 (all variables measured at multiple locations were normalised as in the corresponding test for CH_4 described above).

Emissions of CH_4 and CO_2. The mean CH_4 emission was 8.8 ± 23.5 [0.009–930] mmol m^{-2} d^{-1} (standard deviation and range includes all values, i.e. both spatial and temporal variability; $n_{modelled} = 52332$; uncertainty range for mean 3.5 to 14.0 mmol m^{-2} d^{-1}; assuming an uncertainty of ±60% of mean, see Methods). The mean CO_2 emission was 1600 ± 4800 [3.3–90300] mmol m^{-2} d^{-1} ($n_{modelled} = 52332$; uncertainty range for mean 1200
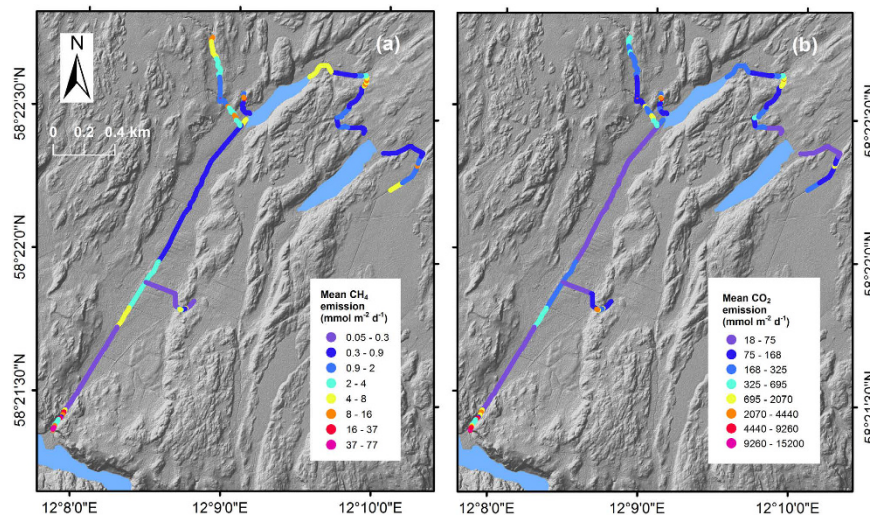
Figure 4. Mean modelled CH_4 (**a**) and CO_2 (**b**) emissions from the streams of SRC showing hotspots for emission. The majority of the streams had low emissions, but some reaches had high emissions due to high k or high concentrations or a combination of both. The figure was created with ArcMap 10.3.1 available from http://www.esri.com/. The background maps, obtained from Lantmäteriet (National Land Survey of Sweden), were published under the copyright agreement i2012/898 with Linköping University.

to 2000 mmol m^{-2} d^{-1}; assuming an uncertainty of $\pm 25\%$ of mean) from all sections (Figs 4 and S4). At location L7, which had the highest mean k_{600}, the mean CH_4 and CO_2 emissions were 3 times higher than the overall mean (Figs S3 and S4). The lowest mean CH_4 emission was observed for L6, which had the lowest CH_4 concentrations, and L5, which had the lowest k_{600} (Figs 3, 4 and S4). L5 also had the lowest mean CO_2 emission (Fig. S4).

The calculated emissions from the gas concentrations and the modelled k_{600} showed good relative agreement with independent measurements used for validation, including mass balance calculations for steep sections from upstream and downstream differences in gas concentrations, and drifting flux chamber emission measurements in flat areas (see Supplementary Information; Table S1 and Fig. S8).

Large temporal variability in emissions of CH_4 and CO_2 were noted (Fig. 5). Stepwise multiple linear regressions of modelled emissions with gas concentrations or k together with all the slope/location categories showed that the CO_2 emissions were largely driven by k as k for CO_2 alone explained 83% of the variations in the emissions over time ($p < 0.001$). This was very different compared to the CH_4 emissions, for which k for CH_4 explained only 50% of the temporal variation ($p < 0.001$). The CH_4 concentrations were a better predictor for CH_4 emissions, as they explained 72% of the variability together with slope categories ($p < 0.001$). The cumulative CH_4 and CO_2 emissions from each of the sections showed higher increments in emissions during high discharge periods (Fig. 5). This pattern was clearer in 2014 and the total annual emissions of CH_4 and CO_2 in 2014 were 1.6 and 2 times higher than in 2013, respectively (Fig. 5).

Discussion

Patterns in gas transfer velocity. High variability in k_{600} among stream sections was observed with very high values for steep sections including small water falls. The mean measured k_{600} from all reaches measured was 67.5 m d^{-1} while the mean k_{600} excluding the high turbulent reaches (B, C and F) was 6.5 m d^{-1}. The mean modelled k_{600} for the entire network, accounting for the relative area distribution as 90.5% of the stream area in the catchment has a slope less than 1% (Table 3), was 21.3 m d^{-1}. Humborg et al.[32] estimated k_{600} for Swedish streams of stream orders 1 to 6 ranging from 6.3 to 15.5 m d^{-1} using equations from O'Connor and Dobbins[33]. Campeau et al.[12] measured mean k_{600} values in the range of 0.6 to 2.3 m d^{-1} in the rivers and streams of a relatively flat landscape in Northern Québec, Canada. Crawford et al.[34] reported k for CO_2 ranging from 0.3 to 13.5 m d^{-1} in the Northern Highlands Lake District, USA. Some other studies, for example Billett and Harvey[27], measured high gas transfer velocities in headwater peatland streams in the UK with a median and mean k of 16.1 and 41.0 m d^{-1}, respectively. Similarly, Butman and Raymond[35] modelled a mean k of 18.0 m d^{-1} for streams and rivers in the relatively steep landscape of western USA. Extreme k_{600} values in the range of 864 to 1848 m d^{-1} were measured in steep rapids of Colorado River, Grand Canyon, USA[36]. Thus, our k_{600} values are largely within the ranges previously estimated in studies of stream reaches having highly different characteristics.

Several models to predict k_{600} from e.g. stream slope and water velocity have been published. When testing if seven such models[15] could reproduce our measured k_{600} values, we found good correspondence at k_{600} levels below 100 m d^{-1}. However, at higher k_{600} levels the models substantially underestimated our measured values (modelled k_{600} was 20–45% of measured k_{600} in the highest range). This could be explained if the previously published models were not based on data for high slope stream sections and therefore not calibrated or validated for high k situations.

Gas concentrations. The range in CH_4 concentrations measured in our study (0.01–46.1 μM; mean–1.7 μM) was within the ranges reported for streams in the literature. Our CH_4 concentrations were higher than the range
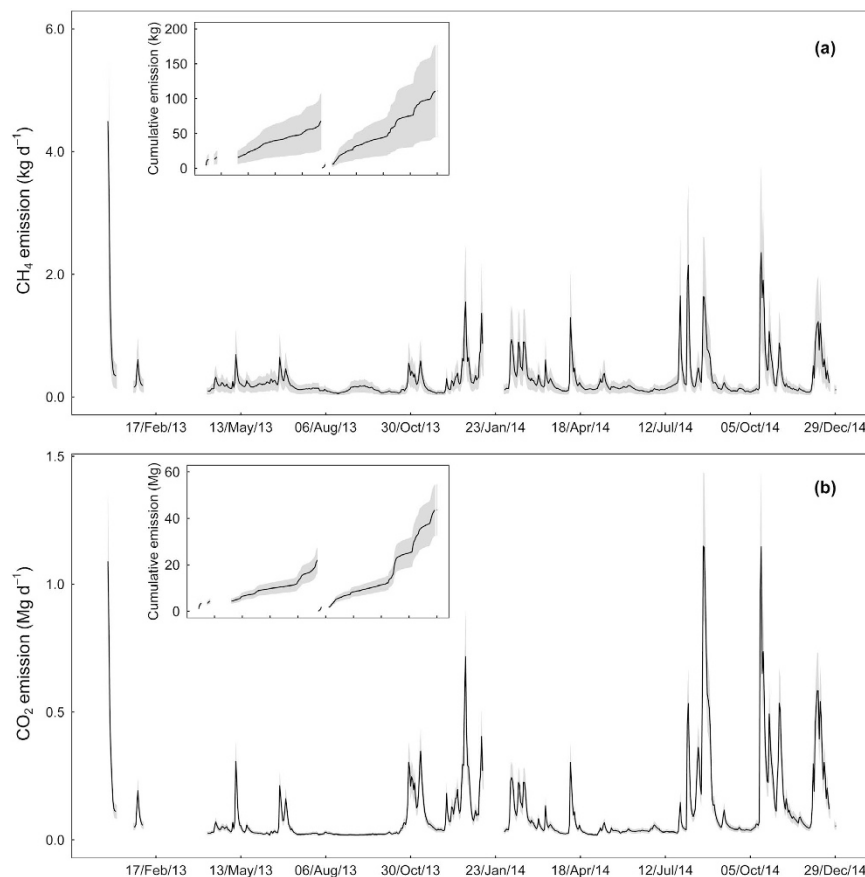
Figure 5. Daily emissions of CH_4 (**a**) CO_2 (**b**) from the studied streams in the two years. The inset panels in (**a,b**) shows the cumulative emissions of the two gases for the corresponding period. The shaded region represents an assumed uncertainty of ± 60 and 25% of mean for CH_4 and CO_2 emissions, respectively (see Methods for details).

(0.2–5.8 μM) measured in the Stordalen catchment, Northern Sweden[9] and in a first order stream (0.04–0.1 μM) in Tennessee, USA[11], but similar to the mean concentrations of 0.05 up to 1.9 μM measured in headwater streams of Scotland[37]. Similar CH_4 concentrations were also reported in studies in boreal region of Northern Québec, Canada (0.04–49.2 μM)[12], in headwater streams of U.K. (0.002–15.3 μM)[27] and in extensive sampling of headwaters in south Sweden (0.16–57.4 μM)[13]. The range in CO_2 concentrations measured in our study (27.5–1124.1 μM) was similar to the range (23.8–714.7 μM) previously reported in many studies in Northern Québec, Canada, U.K. and Sweden[9,12,13,27].

The gas concentrations in stream water represents a net balance between (1) the emission rates from the stream and (2) the input from terrestrial and aquatic sources along the stream network[5,13,18–20,37]. The observed variability in concentrations seemed associated with both these factors. Locations typically surrounded by organic soils (L1, L4 & L5) had higher concentrations which agrees with previous findings[5,19,20,37–39], indicating the importance of terrestrial and wetland gas input. At the same time, low gas concentrations in the high slope reaches indicates that local concentrations within areas with similar input can be regulated by differences in gas loss rates. Given this complex regulation of concentrations for both gases, high resolution monitoring with adequate coverage of spatial variability is needed to develop more accurate modelling of stream CH_4 and CO_2 concentrations[13,32].

CH_4 and CO_2 emissions from the studied streams.

Previous measurements show a wide range of emissions from streams. CH_4 emissions in the range of 0.03 to 0.8 mmol m^{-2} d^{-1} were measured in first order streams in Tennessee, USA[11]. CH_4 emissions ranging from 2.2 to 37.4 mmol m^{-2} d^{-1} in headwaters in Scotland, 0 to 60.1 mmol m^{-2} d^{-1} in small streams in USA, and emissions of 0.8 to 5.0 mmol m^{-2} d^{-1} in headwaters of Alaska have been measured[18,34,37]. Lundin et al.[9] reported mean CH_4 emissions of 15.8 mmol m^{-2} d^{-1} in streams of Northern Sweden. CO_2 emissions from headwater streams of UK and streams of central Germany ranged between 316.1 and 3461.0 mmol m^{-2} d^{-1}[27], and from 23.0 to 355.0 mmol m^{-2} d^{-1}, respectively[40]. Others such as Hope et al.[37] and Crawford et al.[34] have estimated emissions in the range of 21.6 to 3820.0 mmol m^{-2} d^{-1} and −50.0 to 2030.0 mmol m^{-2} d^{-1}, respectively. Mean CO_2 emissions of 1300.0 mmol m^{-2} d^{-1} were reported in streams of Northern Sweden by Lundin et al.[9]. Our emissions (mean CH_4 emission of 8.8 ± 23.5 and mean CO_2 emission of 1600 ± 4800 mmol m^{-2} d^{-1}) were within previously measured ranges, but on the high side which is explained by the organic rich soils in the catchment and that we tried to account for the full spatio-temporal variability in

emissions including high turbulent sections of the stream network, which was important for the total emissions (discussed further below).

The CH_4 emissions reported includes the transport of dissolved CH_4 across the water-air boundary layer (sometimes called diffusive emission). Enhanced emissions of CH_4 via microbubbles have recently been suggested[41,42]. At the concentration levels found in this study CH_4 microbubbles would not form spontaneously, i.e. although there was a supersaturation relative to 2 ppm CH_4 in the air, there was not a supersaturation relative to 100% CH_4. Rapid degassing of both CH_4 and CO_2 into small air bubbles formed in the highly turbulent (e.g. waterfall sections) were integrated in the k values measured, and thereby included in our model. Release of CH_4 bubbles from sediments could only have been captured by the drifting chambers used for model validation but the limited extent in time of these measurements implies that ebullition was not representatively measured. Hence, overall CH_4 emissions may have been underestimated because ebullition was not accounted for.

The general agreement between the three independent methods to estimate emissions–(*i*) modelling from k determined with propane tracer injections combined with water concentrations measurements, (*ii*) mass balance calculations along selected stream sections, and (*iii*) drifting chambers –in spite of highly variable conditions along the stream network, indicates that our measurements and model results are relatively robust (see Supplementary Information; Table S1 and Fig. S8). Approaches (*i*) and (*ii*) should be comparable because both are based on mass balance calculations of gas loss over short stream sections for either the injected propane tracer or in this case CO_2 (which dominates the dissolved inorganic carbon pool in the studied streams). Lower correspondence is expected between approach *(i)* and *(iii)* because drifting chambers measure gas exchange along a specific path of the stream. Additional questions regarding if drifting chambers disturb the water surface have been raised[43], but recent results show that the chamber type used here is suitable for gas flux measurements in both lakes and streams[44,45]. Overall, given the highly variable conditions along streams, careful validation using independent but comparable measurement approaches is recommended.

The variability in emissions was primarily driven by the spatial variability in k (i.e. stream slope and water velocity) and gas concentrations regarding both studied gases. k was relatively more important for CO_2 emissions, while CH_4 emissions seem to be more dependent on the water CH_4 concentrations. This was likely due to the higher variability in CH_4 concentrations making emissions more dependent on concentrations than on k. These differences are important for designing future efforts to better estimate stream emissions, and optimising the resource allocation to k versus concentration monitoring. However, at the local level, both k and concentrations were influenced by discharge with gas import and export. Hence, the difference among years related to discharge is expected and was also noted: discharge in 2014 was 1.7 times higher than in 2013 being consistent with the different emission estimates among the years (Fig. 5).

The total emissions of CH_4 and CO_2 from the studied stream network were estimated to be 89.5 (36.0–143.1) kg yr^{-1} and 32.9 (24.6–41.2) Mg yr^{-1}, respectively, from an area of 6319 m^2 (see Supplementary Information for stream area estimation). In terms of CO_2 equivalents, this was 35.4 (25.6–45.2) Mg yr^{-1} (when assuming a warming potential of CH_4 of 28 over a 100-yr horizon according to Myhre *et al.*[46]), with CH_4 contributing 7%. Previous stream studies have suggested that CH_4 emissions are minor when compared to CO_2[27,38]. However, Crawford *et al.*[34] and Campeau *et al.*[12] reported that CH_4 accounted for 26 and 34% of the total CO_2 equivalents emitted from streams. Our study indicates that CH_4 can contribute substantial CO_2 equivalent emissions from streams, and that the large spatial variability in CH_4 emissions needs consideration in future studies.

The importance of spatio-temporal variability for total emissions.

An analysis of emissions from different slope and discharge categories revealed high emissions in high slope reaches and during high discharge periods (Table 3; Figs 5 and S4). The streams with a slope <1% occupied 90% of the total stream surface area but their mean emissions of CH_4 and CO_2 emissions per m^2 were 5 times lower than the overall mean (Table 3). The slope categories S3, S4 and S5 had emissions higher than the overall mean. The slope category S5, which occupied just 0.9% of the total stream surface area, had areal emissions that were 3 and 4 times higher than the overall mean emissions for CH_4 and CO_2, respectively (Table 3). Therefore, despite the small areal coverage, the slope categories S4 and S5 (which occupied less than 2% of the total steam area), contributed to 18 and 30% of total CH_4 and CO_2 emissions, respectively. However, it has to be noted that our modelled emissions are conservative and underestimated fluxes from highly turbulent/water fall sections (see Supplementary Information and Fig. S8).

Regarding temporal variability, 69% of the days had a stream discharge that was lower or equal to the mean discharge of the two-year study period, but the emissions from this period were lower than the overall mean CH_4 and CO_2 emissions (Table 3). The mean emissions steadily increased as the discharge increased and clearly showed highest emissions during high discharge periods. For example, during days with a discharge greater than 4 times the mean daily discharge, representing 5% of the study period, the mean emissions of CH_4 and CO_2 were more than 3 times the overall mean emissions (Table 3). The high discharge periods, with discharge greater than 3 times the mean daily discharge, occurred less than 10% of the study period, but were responsible for 37 and 43% of total CH_4 and CO_2 emissions, respectively. Had we sampled in more or less flat areas and during moderate flows (ignoring the extremes in both cases), we still could have covered majority of the space and time (90% of area and 69% of time) but arrived at substantially underestimated emissions i.e. the emissions from flat areas and moderate flows were just 55 and 36% of CH_4 emissions and 41 and 26% of CO_2 emissions, respectively. This illustrates the importance of representative sampling and modelling when scaling to the landscape level. Hotspots of degassing along the stream network and high discharge events should be taken into account when possible. Moreover, k values from small areas with high water turbulence should not be extrapolated to large areas because this lead to overestimated emissions.

Given these results, accurate assessments of gas emissions from stream networks depend on consideration of the large spatial variability in both k and concentrations. Although steep sections can have low gas concentrations, their high k can make these sections important for emissions. On a temporal scale, high discharge events are important and a large of part of the annual emissions may happen during these very short periods. Projected

shifts in the hydrological regimes for many regions, as a result of a changing climate, may contribute further to the temporal patterns. The potential importance of the short high discharge periods has been discussed previously, but quantifications of their relative importance are still rare. We conclude that further development of sensor network based measurements and the types of modelling approaches presented here would be beneficial to better account for the hot spots and hot moments in future gas emission assessments.

Methods

Study site. The study was conducted in the Skogaryd Research Catchment (SRC; 58°22′N, 12°9′E), situated in Southwest Sweden (Fig. 1). The 7 km² catchment is mostly covered by forest (58% coniferous forests, 14% mixed forest), dominated by *Picea abies* (L.) H. Karst. and *Pinus sylvestris* L., and to a minor part by agricultural land (9%). About 14% is covered by cleared forest, 4% by mire and 1% by lakes and streams. The annual mean temperature and precipitation were 7.0 °C and 910 mm, respectively, for the years 1983–2013 (Swedish Meteorological and Hydrological Institute; http://luftwebb.smhi.se/). The altitudes in the catchment ranged from 51 to 78 m above the average sea level. The main stem of the stream network originates in a mire just upstream of Lake Erssjön (Fig. 1). Via a chain of streams and lakes (Lake Erssjön and Lake Földjesjön) the main stem drains into the large Lake Skottenesjön (Fig. 1). The network consists of a mixture of flat and slow-flowing areas, especially between the outlet of Lake Földjesjön to Lake Skottenesjön, whereas other parts of the network flow through relatively steep terrain creating small waterfalls and turbulent conditions. The majority of the stream network is affected by man-made ditching conducted 100–150 years ago to improve forest and agricultural productivity.

Measurements of gas transfer velocity (*k*). Gas transfer coefficients (*g*) were determined using injections of a volatile gas tracer, propane (C_3H_8), as described in similar studies[11,14,37,47] and in the Supplementary Information. Six stream reaches ranging in length from 20 to 54 m (Fig. 1 and Table 1) were chosen to represent end-members in morphological conditions of the streams within the catchment. The reaches A, D and E are straight ditches with gentle slope (<1.5%) whereas the reaches B, C and F represent relatively steep (>7.5%) and highly turbulent stream sections (Fig. 1 and Table 1).

The gas exchange coefficients of propane ($g_{C_3H_8}$) from the tracer injections were calculated according to Genereux and Hemond[48] using the modification suggested by Wallin *et al.*[14] to correct for the dilution by groundwater inputs along the study reach according to

$$g_{C_3H_8} = \frac{1}{\tau} \times \ln\left(\frac{[C_3H_8]_U \times Q_U}{[C_3H_8]_D \times Q_D}\right)$$

(1)

where $g_{C_3H_8}$ is the gas transfer coefficient of propane (min⁻¹), τ is the reach travel time (min), $[C_3H_8]_U$ and $[C_3H_8]_D$ are the relative concentrations of propane in the upstream and downstream samples, respectively, and Q_U and Q_D are the discharge (L s⁻¹) at the upstream and downstream stations, respectively. The difference in the upstream and downstream discharge calculated from the estimated discharge (see below) ranged from 0.06 to 0.5%, and this was used to calculate Q_U and Q_D from the measured mean discharge. The $g_{C_3H_8}$ was converted to gas transfer velocities (*k*; m d⁻¹) by multiplication with the average stream depth of the reach at each sampling occasion. An alternative approach to derive *k* from the general diffusive flux calculation[49]

$$F = k(C_{aq} - C_{eq}),$$

(2)

where F is the flux to the atmosphere–here determined as the loss of propane from a water section during the reach travel time, C_{aq} is the water concentrations as measured and C_{eq} is the theoretical water concentration in equilibrium with the atmospheric partial pressure according to Henry's Law, yielded almost identical *k* values.

The *k* values for propane were converted to k_{600} (i.e. *k* for a gas having the Schmidt number of 600; this corresponds to the *k* for CO_2 in freshwater at 20 °C) to enable comparison across temperatures and different gases according to Wanninkhof[50] as

$$k_{600} = k\left(\frac{600}{Sc}\right)^{-0.5}$$

(3)

where *k* denotes the gas transfer velocity (m d⁻¹) and *Sc* is the Schmidt number of the gas in focus according to Wanninkhof[31]. *Sc* for propane was calculated as described in Raymond *et al.*[15]. We found a discrepancy in temperature dependent diffusion coefficients for propane in the literature[51,52], in turn leading to alternative Schmidt numbers having a clear impact on the outcome of the emission calculations. We used the diffusion coefficients from Wise and Houghton[52] which were determined in a relevant temperature interval, have been widely used previously, and resulted in the best fit between our emission model and the independent gas emission measurements used for validation (Figs 2 and S8).

The k_{600} values were converted to gas and temperature specific *k*-values for CO_2 and CH_4 according to

$$k_g = k_{600}\left(\frac{Sc_g}{600}\right)^{-0.5}$$

(4)

where k_g and Sc_g denote k and Sc for a specific gas (here CO_2 or CH_4) at a specific temperature (the water temperature during the time period in focus). Stream velocity (m s^{-1}) for each tracer injection was calculated by dividing the length of the reach by the reach travel time (see Supplementary Information).

Measurements of stream water CH_4 and CO_2 concentrations.

CO_2 concentrations. The CO_2 concentrations in the stream network were measured using plastic chambers equipped with CO_2 sensors (CO_2 Engine® ELG, SenseAir AB, Sweden; range 0–10000 ppm) described in detail in Bastviken *et al.*[53] (see Supplementary Information for details). In 2013, 8 chambers were used at different locations in the stream network (Fig. 1). Due to practical constraints in using chambers for long-term deployments (rapid changes in water level, dry season with little water, storm events with rapid water flow etc.) there were data gaps. In 2014, 20 chambers were used to obtain a better spatial representation. The data from the sensors were filtered to remove condensation peaks[53] by removing values greater than 20% of 12 hour averages before and after each measurement. A total of 28,463 CO_2 measurements were made in the two years.

CH_4 measurements. The CH_4 concentrations were determined by a headspace equilibration method[54] (see Supplementary Information for a description). The concentrations of CH_4 in the stream water were measured approximately every two weeks in 2013 (May-Nov) and 2014 (Apr-Nov) at four monitoring stations whose locations are given in Fig. 1. In 2014, CH_4 concentrations were also measured close to the CO_2 chamber measurements to better cover the spatial variability. CH_4 concentrations measured during the propane injections were included in the data analysis. A total of 292 stream water CH_4 concentration measurements were conducted during the study period. Additional details on gas analysis using a gas chromatograph are given in the Supplementary Information.

Stream network k estimates.

A digital elevation model (DEM) of the catchment with a 2 m horizontal resolution was obtained from Lantmäteriet (https://maps.slu.se/get/). The stream network of the catchment and the overall and partial drainage areas were extracted from the DEM using the Spatial Analyst toolbox in ArcGIS 10.3. The daily discharge for each 2 m stream section, out of the, in total, 6.4 km long stream network was estimated as follows: (1) Stream discharge was measured at four monitoring stations in the catchment according to the methodology described by Wallin *et al.*[55] (see also Supplementary Information). From these measurements we generated daily average discharge at four locations in the stream network. (2) The upstream drainage area for each of the four stations were determined using the Spatial Analyst toolbox in ArcGIS 10.3. (3) Hence, for each day we could make a regression equation, $D = bA$, where D is discharge, A is upstream drainage area, and b is a constant (i.e., the average discharge per unit area), based on the discharge data for the specific day from the four stations. The study encompassed 623 days (January 2013 to December 2014, except during periods when average air temperatures were below 0 °C for more than 3 days in a row and discharge measurements indicated that streams were frozen), meaning that 623 separate such equations valid for their respective day were made. R^2 exceeded 0.92 for all days (average 0.98). The range of b was 0.2 to 315. (4) The upstream drainage area for each 2 m stream section was determined from ArcGIS and was multiplied with b of the 623 equations to estimate average daily discharge for each such 2 m section.

The stream network was divided into 84 reaches where the length of each reach was defined by an elevation difference of 0.5 m. The slopes (%) of the stream reaches were calculated by dividing the elevation difference of each reach by the reach length.

We established a regression model with velocity as a function of discharge and slope measured in the stream reaches where tracer injections were conducted (Table 2). This model was used to extrapolate the velocity for all 84 stream reaches from January 2013 to December 2014 using daily reach average discharge and slope for each individual stream reach. k_{600} values in the whole stream network were then modelled from stream slope and water velocity as predictor variables (see Fig. S9 for a brief summary of methods).

Emission estimates for the stream network.

Emissions were calculated by using Eq. 2. Daily emissions were calculated for each of the 84 reaches, using reach specific daily k estimates. No good relationship between CH_4 and CO_2 concentrations and any independent variables were found (see Results), thus modelling spatially distributed CH_4 and CO_2 concentrations at a daily time step was not possible. Instead, CO_2 and CH_4 concentrations in the un-sampled reaches were estimated, based on manual concentration measurements from 20 points of the stream network (measurements done on 5 occasions for CH_4 and 7 for CO_2 in 2014). Concentrations were interpolated between these 20 points (e.g. assuming linear change in concentration between upstream and downstream measurements when available). The ratios of the interpolated concentrations in relation to the concentrations at the most frequently samples measurement points of CH_4 and CO_2 were then calculated, yielding relative concentrations in each stream reach. Assuming that these relative concentrations were valid for the time periods between the spatially resolved samplings, the concentration levels in each reach over time were estimated from the concentrations at the temporally resolved sampling points (biweekly for CH_4 and daily mean for CO_2). For the days between sampling occasions, concentrations were linearly interpolated to gap-fill. Daily emissions for each of the 84 reaches were then calculated based on the stream surface area of each reach (expressed in kg d^{-1} for CH_4 and Mg d^{-1} for CO_2). The emissions from all 84 reaches were then summed and total emissions of CH_4 and CO_2 from the streams were expressed in kg yr^{-1} or Mg yr^{-1}. By far the largest uncertainty in the emission estimates come from the relative concentration ratios used to represent spatial differences along the streams during the different periods to interpolate concentrations within the stream network. Therefore, the coefficient of variations (CV) of the interpolation ratios of each reach were calculated and the maximum CV was used to estimate uncertainty range for the mean for all reaches, which were 60 and 25% for CH_4 and CO_2 emissions, respectively.

Data analyses. Residuals in the linear regressions were checked for normal distribution and randomness of errors and the original variables were $\log_{10}$ transformed when this criterion was not met. The predicted values from the $\log_{10}$ transformed linear regression equations were back transformed to original units using the correction proposed by Newman[56]. The concentrations, k_{600} and emissions for CO_2 and CH_4 were divided into seven groups based on location (L1 to L7; referred to as location categories; see Fig. 1) and into five groups based on slope (S1 (0–1%), S2 (1–2%), S3 (2–4%), S4 (4–6%) and S5 (6–21%); referred to as slope categories). For CH_4 and CO_2 concentrations, slope categories were based on the slope of the reach where the measurement points were located. A univariate General Linear Model (GLM) with Tukey's post hoc test was used, with location and slope categories as factors, to analyse spatial variability. All statistical analyses were done in IBM SPSS Statistics 23 (IBM Corp., USA) with a significance level of 0.05. GIS related analyses were performed in ArcGIS 10.3 (Esri Inc., USA).

References

1. Bastviken, D., Tranvik, L. J., Downing, J. A., Crill, P. M. & Enrich-Prast, A. Freshwater methane emissions offset the continental carbon sink. *Science* **331,** 50 (2011).
2. Raymond, P. A. *et al.* Global carbon dioxide emissions from inland waters. *Nature* **503,** 355–359 (2013).
3. Aufdenkampe, A. *et al.* Riverine coupling of biogeochemical cycles between land, oceans, and atmosphere. *Front. Ecol. Environ.* **9,** 53–60 (2011).
4. Cole, J. J. *et al.* Plumbing the Global Carbon Cycle: Integrating Inland Waters into the Terrestrial Carbon Budget. *Ecosystems* **10,** 172–185 (2007).
5. Borges, A. V. *et al.* Divergent biophysical controls of aquatic CO_2 and CH_4 in the World's two largest rivers. *Scientific Reports* **5,** 15614, doi: 10.1038/srep15614 (2015).
6. Stanley, E. H. *et al.* The ecology of methane in streams and rivers: Patterns, controls, and global significance. *Ecol. Monogr.* **86,** 146–171 (2016).
7. Ciais, P. *et al.* In *Climate Change 2013: The Physical Science Basis. Contribution of Working Group I to the Fifth Assessment Report of the Intergovernmental Panel on Climate Change* (eds T. F. Stocker *et al.*) 465–570 (Cambridge University Press, 2013).
8. Koprivnjak, J. F., Dillon, P. J. & Molot, L. A. Importance of CO_2 evasion from small boreal streams. *Global Biogeochem. Cycles* **24,** GB4003, doi: 10.1029/2009gb003723 (2010).
9. Lundin, E. J., Giesler, R., Persson, A., Thompson, M. S. & Karlsson, J. Integrating carbon emissions from lakes and streams in a subarctic catchment. *J. Geophys. Res.: Biogeosci.* **118,** 1200–1207 (2013).
10. Teodoru, C. R., Del Giorgio, P. A., Prairie, Y. T. & Camire, M. Patterns in pCO₂ in boreal streams and rivers of northern Quebec, Canada. *Global Biogeochem. Cycles* **23,** GB2012, doi: 10.1029/2008gb003404 (2009).
11. Jones, J. B. & Mulholland, P. J. Methane input and evasion in a hardwood forest stream: Effects of subsurface flow from shallow and deep pathways. *Limnol. Oceanogr.* **43,** 1243–1250 (1998).
12. Campeau, A., Lapierre, J.-F., Vachon, D. & del Giorgio, P. A. Regional contribution of CO_2 and CH_4 fluxes from the fluvial network in a lowland boreal landscape of Québec. *Global Biogeochem. Cycles* **28,** 57–69 (2014).
13. Wallin, M. B., Lofgren, S., Erlandsson, M. & Bishop, K. Representative regional sampling of carbon dioxide and methane concentrations in hemiboreal headwater streams reveal underestimates in less systematic approaches. *Global Biogeochem. Cycles* **28,** 465–479 (2014).
14. Wallin, M. B. *et al.* Spatiotemporal variability of the gas transfer coefficient (KCO_2) in boreal streams: Implications for large scale estimates of CO_2 evasion. *Global Biogeochem. Cycles* **25,** GB3025, doi: 10.1029/2010gb003975 (2011).
15. Raymond, P. A. *et al.* Scaling the gas transfer velocity and hydraulic geometry in streams and small rivers. *Limnol. Oceanogr.: Fluids Environ.* **2,** 41–53 (2012).
16. Long, H. *et al.* Hydraulics are a first order control on CO_2 efflux from fluvial systems. *J. Geophys. Res.: Biogeosci.* **120,** 1912–1922 (2015).
17. Hope, D., Palmer, S. M., Billett, M. F. & Dawson, J. J. C. Variations in dissolved CO_2 and CH4 in a first-order stream and catchment: an investigation of soil-stream linkages. *Hydrol. Processes* **18,** 3255–3275 (2004).
18. Crawford, J. T., Striegl, R. G., Wickland, K. P., Dornblaser, M. M. & Stanley, E. H. Emissions of carbon dioxide and methane from a headwater stream network of interior Alaska. *J. Geophys. Res.: Biogeosci.* **118,** 482–494 (2013).
19. Abril, G. *et al.* Amazon River carbon dioxide outgassing fuelled by wetlands. *Nature* **505,** 395–398 (2014).
20. Borges, A. V. *et al.* Globally significant greenhouse-gas emissions from African inland waters. *Nat. Geosci.* **8,** 637–642 (2015).
21. Teodoru, C. R. *et al.* Dynamics of greenhouse gases (CO_2, CH_4, N_2O) along the Zambezi River and major tributaries, and their importance in the riverine carbon budget. *Biogeosciences* **12,** 2431–2453 (2015).
22. Wallin, M., Buffam, I., Öquist, M., Laudon, H. & Bishop, K. Temporal and spatial variability of dissolved inorganic carbon in a boreal stream network: Concentrations and downstream fluxes. *J. of Geophys. Res.: Biogeosci.* **115,** G02014, doi: 10.1029/2009jg001100 (2010).
23. Roberts, B. J., Mulholland, P. J. & Hill, W. R. Multiple scales of temporal variability in ecosystem metabolism rates: Results from 2 years of continuous monitoring in a forested headwater stream. *Ecosystems* **10,** 588–606 (2007).
24. Dinsmore, K. J. *et al.* Contrasting CO_2 concentration discharge dynamics in headwater streams: A multi-catchment comparison. *J. Geophys. Res.: Biogeosci.* **118,** 445–461 (2013).
25. Dinsmore, K. J. & Billett, M. F. Continuous measurement and modeling of CO_2 losses from a peatland stream during stormflow events. *Water Resour. Res.* **44,** W12417 (2008).
26. Dyson, K. E. *et al.* Release of aquatic carbon from two peatland catchments in E. Finland during the spring snowmelt period. *Biogeochemistry* **103,** 125–142 (2011).
27. Billett, M. F. & Harvey, F. H. Measurements of CO_2 and CH_4 evasion from UK peatland headwater streams. *Biogeochemistry* **114,** 165–181 (2013).
28. Peter, H. *et al.* Scales and drivers of temporal pCO₂ dynamics in an Alpine stream. *J. Geophys. Res.: Biogeosci.* **119,** 1078–1091 (2014).
29. Lauerwald, R., Laruelle, G. G., Hartmann, J., Ciais, P. & Regnier, P. A. G. Spatial patterns in CO_2 evasion from the global river network. *Global Biogeochem. Cycles* **29,** 534–554 (2015).
30. Abril, G. *et al.* Technical Note: Large overestimation of pCO₂ calculated from pH and alkalinity in acidic, organic-rich freshwaters. *Biogeosciences* **12,** 67–78 (2015).
31. Wanninkhof, R. Relationship between wind speed and gas exchange over the ocean revisited. *Limnol. Oceanogr.: Methods* **12,** 351–362 (2014).
32. Humborg, C. *et al.* CO_2 supersaturation along the aquatic conduit in Swedish watersheds as constrained by terrestrial respiration, aquatic respiration and weathering. *Global Change Biol.* **16,** 1966–1978 (2010).
33. O'Connor, D. J. & Dobbins, W. E. Mechanisms of reaeration in natural streams. *Trans. Am. Soc. Civ. Eng.* **123,** 641–666 (1958).
34. Crawford, J. T. *et al.* CO_2 and CH_4 emissions from streams in a lake-rich landscape: Patterns, controls, and regional significance. *Global Biogeochem. Cycles* **28,** 197–210 (2014).

35. Butman, D. & Raymond, P. A. Significant efflux of carbon dioxide from streams and rivers in the United States. *Nat. Geosci.* **4,** 839–842 (2011).
36. Hall, R. O., Kennedy, T. A. & Rosi-Marshall, E. J. Air–water oxygen exchange in a large whitewater river. *Limnol. Oceanogr.: Fluids Environ.* **2,** 1–11 (2012).
37. Hope, D., Palmer, S. M., Billett, M. F. & Dawson, J. J. C. Carbon dioxide and methane evasion from a temperate peatland stream. *Limnol. Oceanogr.* **46,** 847–857 (2001).
38. Dinsmore, K. J. *et al.* Role of the aquatic pathway in the carbon and greenhouse gas budgets of a peatland catchment. *Global Change Biol.* **16,** 2750–2762 (2010).
39. Billett, M. F. & Moore, T. R. Supersaturation and evasion of CO_2 and CH_4 in surface waters at Mer Bleue peatland, Canada. *Hydrol. Processes* **22,** 2044–2054 (2008).
40. Halbedel, S. & Koschorreck, M. Regulation of CO_2 emissions from temperate streams and reservoirs. *Biogeosciences* **10,** 7539–7551 (2013).
41. McGinnis, D. F. *et al.* Enhancing Surface Methane Fluxes from an Oligotrophic Lake: Exploring the Microbubble Hypothesis. *Environ. Sci. Technol.* **49,** 873–880 (2015).
42. Prairie, Y. T. & del Giorgio, P. A. A new pathway of freshwater methane emissions and the putative importance of microbubbles. *Inland Waters* **3,** 311–320 (2013).
43. Raymond, P. A. & Cole, J. J. Gas exchange in rivers and estuaries: Choosing a gas transfer velocity. *Estuaries* **24,** 312–317 (2001).
44. Lorke, A. *et al.* Technical note: drifting versus anchored flux chambers for measuring greenhouse gas emissions from running waters. *Biogeosciences* **12,** 7013–7024 (2015).
45. Gålfalk, M., Bastviken, D., Fredriksson, S. & Arneborg, L. Determination of the piston velocity for water-air interfaces using flux chambers, acoustic Doppler velocimetry, and IR imaging of the water surface. *J. Geophys. Res.: Biogeosci.* **118,** 770–782 (2013).
46. Myhre, G. *et al.* In *Climate Change 2013: The Physical Science Basis. Contribution of Working Group I to the Fifth Assessment Report of the Intergovernmental Panel on Climate Change* (eds T. F. Stocker *et al.*) 659–740 (Cambridge University Press, 2013).
47. Marzolf, E. R., Mulholland, P. J. & Steinman, A. D. Improvements to the Diurnal Upstream–Downstream Dissolved Oxygen Change Technique for Determining Whole-Stream Metabolism in Small Streams. *Can. J. Fish. Aquat. Sci.* **51,** 1591–1599 (1994).
48. Genereux, D. P. & Hemond, H. F. Naturally-Occurring Rn-222 as a Tracer for Streamflow Generation–Steady-State Methodology and Field Example. *Water Resour. Res.* **26,** 3065–3075 (1990).
49. Liss, P. S. & Slater, P. G. Flux of Gases across the Air-Sea Interface. *Nature* **247,** 181–184 (1974).
50. Wanninkhof, R. Relationship between Wind-Speed and Gas-Exchange over the Ocean. *J. Geophys. Res.: Oceans* **97,** 7373–7382 (1992).
51. Witherspoon, P. A. & Saraf, D. N. Diffusion of Methane, Ethane, Propane, and n-Butane in Water from 25 to 43°. *The Journal of Physical Chemistry* **69,** 3752–3755 (1965).
52. Wise, D. L. & Houghton, G. The diffusion coefficients of ten slightly soluble gases in water at 10–60 °C. *Chem. Eng. Sci.* **21,** 999–1010 (1966).
53. Bastviken, D., Sundgren, I., Natchimuthu, S., Reyier, H. & Gålfalk, M. Technical Note: Cost-efficient approaches to measure carbon dioxide (CO_2) fluxes and concentrations in terrestrial and aquatic environments using mini loggers. *Biogeosciences* **12,** 3849–3859 (2015).
54. McAuliffe, C. G.C. determination of solutes by multiple phase equilibration. *Chem. Tech.* **1,** 46–51 (1971).
55. Wallin, M. B. *et al.* Temporal control on concentration, character, and export of dissolved organic carbon in two hemiboreal headwater streams draining contrasting catchments. *J. Geophys. Res.: Biogeosci.* **120,** 832–846 (2015).
56. Newman, M. C. Regression analysis of log-transformed data: Statistical bias and its correction. *Environ. Toxicol. Chem.* **12,** 1129–1133 (1993).

Acknowledgements

Author Contributions

S.N., M.B.W. and D.B. designed the study; S.N. conducted the field work, analysed the data; S.N. wrote the first draft of the manuscript with major contributions from M.B.W., D.B. and L.K. All authors commented and contributed to the revisions of the manuscript.

Additional Information

Supplementary information accompanies this paper at http://www.nature.com/srep

Competing financial interests: The authors declare no competing financial interests.

How to cite this article: Natchimuthu, S. *et al.* Spatio-temporal patterns of stream methane and carbon dioxide emissions in a hemiboreal catchment in Southwest Sweden. *Sci. Rep.* **7,** 39729; doi: 10.1038/srep39729 (2017).

Publisher's note: Springer Nature remains neutral with regard to jurisdictional claims in published maps and institutional affiliations.